Facile and Controlled Synthesis of 3D Nanorods-Based Urchinlike and Nanosheets-Based Flowerlike Cobalt Basic Salt Nanostructures

ARTICLE *in* THE JOURNAL OF PHYSICAL CHEMISTRY C · MARCH 2007

Impact Factor: 4.77 · DOI: 10.1021/jp067320a

4 AUTHORS:

Zhigang Zhao
Chinese Academy of Sciences
27 PUBLICATIONS **348** CITATIONS
SEE PROFILE

Fengxia Geng
Soochow University (PRC)
34 PUBLICATIONS **753** CITATIONS
SEE PROFILE

Jinbo Bai
Ecole Centrale Paris
170 PUBLICATIONS **4,010** CITATIONS
SEE PROFILE

Hui-Ming Cheng
Shenyang National Laboratory for Materials …
490 PUBLICATIONS **33,764** CITATIONS
SEE PROFILE

Facile and Controlled Synthesis of 3D Nanorods-Based Urchinlike and Nanosheets-Based Flowerlike Cobalt Basic Salt Nanostructures

Zhigang Zhao,[†,‡] Fengxia Geng,[†] Jinbo Bai,[‡] and Hui-Ming Cheng*[,†]

Shenyang National Laboratory for Materials Science, Institute of Metal Research, Chinese Academy of Sciences, 72 Wenhua Road, Shenyang 110016, P. R. China, and Laboratory of Mechanics of Soils, Structures and Materials, CNRS UMR 8579, Ecole Central Paris, 92295 Chatenay-Malabry, France

Received: November 6, 2006; In Final Form: January 2, 2007

We report the controlled synthesis of four kinds of cobalt basic salts with different morphologies and colors (pink, blue, green, and lavender) using urea as a hydrolysis agent in the presence of block copolymer P123. Li_2SO_4 and LiCl were used as salt additives to control the type of cobalt basic salts. It was found that the amount of urea plays a critical role in the synthesis of cobalt basic salts with different phases. Two of them exhibit interesting three-dimensional urchinlike and flowerlike morphology assembled from nanorods (pink) and nanosheets (blue), respectively. The present work suggests that it is possible to directly grow three-dimensional-ordered assemblies built from one-dimensional or two-dimensional cobalt basic salt nanostructures through a one-step aqueous solution-phase chemical route under controlled conditions.

Introduction

Inspired by the formation process of biominerals, it has been an intensive focus to synthesize organized inorganic structures with complex architecture on the basis of the assembly of low-dimensional nanostructured building blocks owing to the importance and potential to design new materials and devices for various application fields such as catalysis, medicine, electronics, pigments, and cosmetics.[1−4] A few strategies have been developed to spatially pattern and control high-order organization, including chemical and microfabrication methods, molecular cross-linking, a DNA-based method, and self-assembly formation of superlattices.[1−4] Alternatively, a variety of organized complex structures with novel morphologies of $CaCO_3$,[4] $BaSO_4$,[5] $BaCrO_4$,[5−6] $BaCO_3$,[7] and so forth have been synthesized.

Cobalt basic salts, expressed using a general formula of $Co(OH)_{2-x}(A^{n-})_{x/n}{\cdot}mH_2O$ (A: Cl^-, NO_3^-, SO_4^{2-}, CO_3^{2-}, etc.), have been extensively studied over the last two decades because of the important electric, magnetic, and catalytic properties of their metal oxides formed upon their thermal decomposition.[8−10] Furthermore, in view of their possible applications as catalysts, anion exchangers, and electrodes for alkaline secondary cells, cobalt basic salts have attracted considerable attention.[11] Compositionally, these represent a series of solid solutions whose end members are $Co(OH)_2$ and Co_nA_2. Structurally, the hydroxyl-rich phases, which are associated with the α-hydroxides, adopt structures isotypic with mineral hydrotalcite, which consists of positively charged $Co(OH)_{2-x}$ layers with anions and water molecules residing in the gallery to restore charge neutrality, while the anion-rich phases adopt a structure of lower symmetry. In all these compounds, the Co^{2+} ion occupies octahedral sites. The coordinative unsaturation of the metal ions is satisfied by the anions, which are grafted directly to the metal ion. Their interlayer spacing is expanded and dependent on the size of the anion.[12] The synthesis of cobalt basic salts usually involves homogeneous precipitation of metal salts with alkaline and the desired anion at a constant pH in the range of 7−9.[13−14] There is a considerable degree of interest in evolving an accelerated chemical route to cobalt basic salts with different forms, even their nanostructures.[10−16] Hosono et al. fabricated films of brucite-type cobalt hydroxide with nanorod morphology and hydrotalcite-type cobalt hydroxide with nanosheet morphology by heterogeneous nucleation in a chemical bath using water and a mixed solution of water−methanol as solvent, respectively.[15] However, the samples synthesized were poorly crystalline. Liu et al. obtained brucite-type and hydrotalcite-type cobalt hydroxide platelets with high crystallinity.[16] At the same time, some reported on the synthesis of nickel basic salts with different forms.[17−18] Liu et al. presented a simple hydrothermal method to obtain new and stable turbostratic α-$Ni(OH)_2$ organic−inorganic hybrid material with adjustable *d* spacing by introducing different anions and hexamethyltetramine, formulated as $Ni(OH)_{2-x}(A^{n-})_{x/n}-(C_6H_{12}N_4)_y{\cdot}zH_2O$.[17] However, to the best of our knowledge, there are few reports concerning the assembly of cobalt basic salt nanostructures into hierarchical organized structures. It remains a significant challenge to develop facile, mild, and effective methods for creating hierarchical architectures assembled from low-dimensional cobalt basic salt nanostructures. Herein, we develop an environmentally benign, aqueous solution-based method to synthesize four kinds of cobalt basic salts with different colors (pink, blue, green, and lavender) in the presence of block copolymer P123. Li_2SO_4 and LiCl were used as salt additives to control the type of cobalt basic salts. Two of them exhibit interesting three-dimensional (3D) urchinlike and flowerlike morphology assembled from nanorods and nanosheets (pink and blue), respectively. The present work suggests that it is possible to directly grow 3D-ordered assemblies built from one-dimensional (1D) and two-dimensional (2D) cobalt basic salt nanostructures through a one-step aqueous solution-phase chemical route under controlled conditions.

* To whom correspondence should be addressed. Tel: 86-24-2397 1611. Fax: 86-24-2390 3126. E-mail: cheng@imr.ac.cn.
† Institute of Metal Research.
‡ Ecole Central Paris.

10.1021/jp067320a CCC: $37.00
Published on Web 02/17/2007

Experimental Section

Chemicals. Block copolymers, which are polymers formed by connecting two or more chemically distinct segments (or blocks) end-to-end with a covalent bond, can often spontaneously self-assemble into various organized nanoscale micelles driven by diverse repulsion forces between the segments.[19] So, they have been recently adapted as water-soluble polymeric templates for the biomimetic synthesis of inorganic nanostructures. Pluronic P123, purchased from Aldrich, is a water-soluble poly(ethylene oxide)-poly(propylene oxide)-poly(ethylene oxide)-based amphiphilic triblock copolymer, with the composition of $EO_{20}PO_{70}EO_{20}$ ($M_{av} = 5800$). The hydrophilic block (EO) of P123 can interact strongly with specific inorganic ions through physical adsorption or chemical coordination, while another hydrophobic block (PO) can mainly promote solubilization in water. All chemicals were of analytical grade and were used as received without further purification. The water used in this work was distilled and deionized.

Synthesis Procedures. In a typical synthesis of nanorod-based urchinlike 3D self-assembled cobalt basic salt nanostructures, a certain amount of triblock copolymer surfactant Pluronic P123 was ultrasonically dispersed in distilled water to form homogeneous micelles. Then, 100 mL precursor aqueous solution of $CoCl_2 \cdot 6H_2O$ (0.05 M) and 100 mL 1 M urea were added into the above P123 aqueous solution with [P123]/[H_2O] weight ratio of 0.04, with vigorous stirring for 30 min to obtain a homogeneous solution. The resulting microemulsion solution was refluxed at 95 °C for 24 h, and a suspension containing pink particles can be observed during refluxing. The suspension obtained was naturally cooled to room temperature and was stored at a constant temperature of 25 °C. After 24 h of aging, pink solid product was collected by centrifugation, was washed with ethanol and distilled water several times, and then was dried in vacuum at 80 °C for 24 h. Finally, these urchinlike nanostructures were harvested. In a typical synthesis of nanosheet-based flowerlike nanostructures (blue sample), the synthetic procedure was similar to the above except that Li_2SO_4 was added into the precursor aqueous solution. For the synthesis of green sample, the synthetic procedure was also similar except that the concentration of urea was decreased to 0.1 M and Li_2SO_4 was substituted by LiCl. For the lavender-colored sample, the concentration of LiCl was significantly increased to 3 M.

Characterization. The obtained samples were characterized by X-ray diffraction (XRD, Shimadzu XRD-6000, Cu Kα radiation). Transmission electron microscopy (TEM) with selected area electron diffraction (SAED) and high-resolution transmission electron microscopy (HRTEM) were performed on JEM-2010F high-resolution transmission electron microscope. For this case, some samples were dispersed in ethanol followed by ultrasonication, and then two small drops of them were placed on a Cu microgrid. The acceleration voltage was 200 kV. Scanning electron microscopy (SEM) images were taken on a LEO 1530 FEG scanning electron microscope. The infrared spectra were obtained on a Fourier transformed infrared spectrometer (FTIR Bruker IFS 55), and thermogravimetric analysis (TGA) was carried out on a TGA-50 thermal analyzer with a heating rate of 10 °C min^{-1} in flowing air.

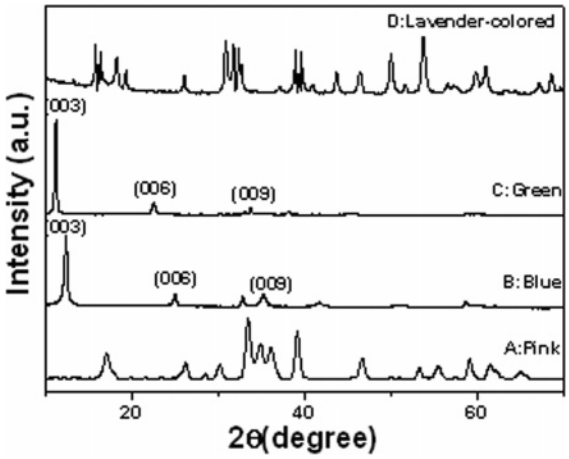

Figure 1. XRD patterns of as-prepared cobalt basic salt compounds.

Results and Discussion

Synthesis of Cobalt Basic Salts. When heated in aqueous solution, urea liberates hydroxyl ions slowly to promote the precipitation of Co^{2+} in $CoCl_2 \cdot 6H_2O$ solution, as described by the following formulation:

$$CO(NH_2)_2 + 3H_2O \rightarrow 2NH_4^+ + 2OH^- + CO_2 \quad (1)$$

CO_3^{2-}, SO_4^{2-}, and Cl^- are used as counter anions. The urea hydrolysis can provide both carbonate and hydroxyl anions to form cobalt hydroxide carbonate. Li_2SO_4 was added into the system to get cobalt hydroxysulfate. However, the obtained cobalt hydroxychloride was not of good quality when LiCl was used in equal molar amounts to substitute for the Li_2SO_4. Two alternate routes were explored. In the first route, the dosage of urea was significantly decreased while that of LiCl was kept unchanged; in the second route, the dosage of LiCl was significantly increased while that of urea was kept unchanged. The OH^- deficit model can explain why the decrease of urea addition is favorable for the formation of pure chloride-intercalating hydrotalcite-like phase, since hydroxyl vacancies can bring positive charges of the layers and the ions can more easily intercalate the layers to restore charge neutrality. Table 1 lists the experimental conditions and the nature of the products obtained. From sample A to D, the product is pink, blue, green, and lavender, respectively. The color change of these samples also reflects the phase change. Blue and green are the typical color of hydrotalcite-like phase α-$Co(OH)_2$ which will be discussed in detail later.

XRD analysis was adopted to analyze the crystal structure and phase composition of the products obtained. Figure 1 shows

TABLE 1: Sample Nomenclature and Experimental Conditions

sample	A (cobalt chloride carbonate hydroxide hydrate)	B (SO_4^{2-}-intercalated α-$Co(OH)_2$)	C (Cl^--intercalated α-$Co(OH)_2$)	D (cobalt hydroxychloride)
dosage of $CoCl_2$ (mol/L)	0.05	0.05	0.05	0.05
dosage of urea (mol/L)	1	1	0.1	1
salt/dosage (mol/L)	no	Li_2SO_4	LiCl	LiCl
		0.05	0.05	3
color	pink	blue	green	lavender
formula	$Co(OH)_{1.10}Cl_{0.2}(CO_3)_{0.35} \cdot 1.74H_2O$	$Co(OH)_{1.82}(SO_4)_{0.09}$ $1.37H_2O$	$Co(OH)_{1.81}Cl_{0.19}$ $1.12H_2O$	$Co_2(OH)_3Cl$
morphology	well-crystallized nanorods	well-crystallized nanosheets	lamellar structure	lamellar structure

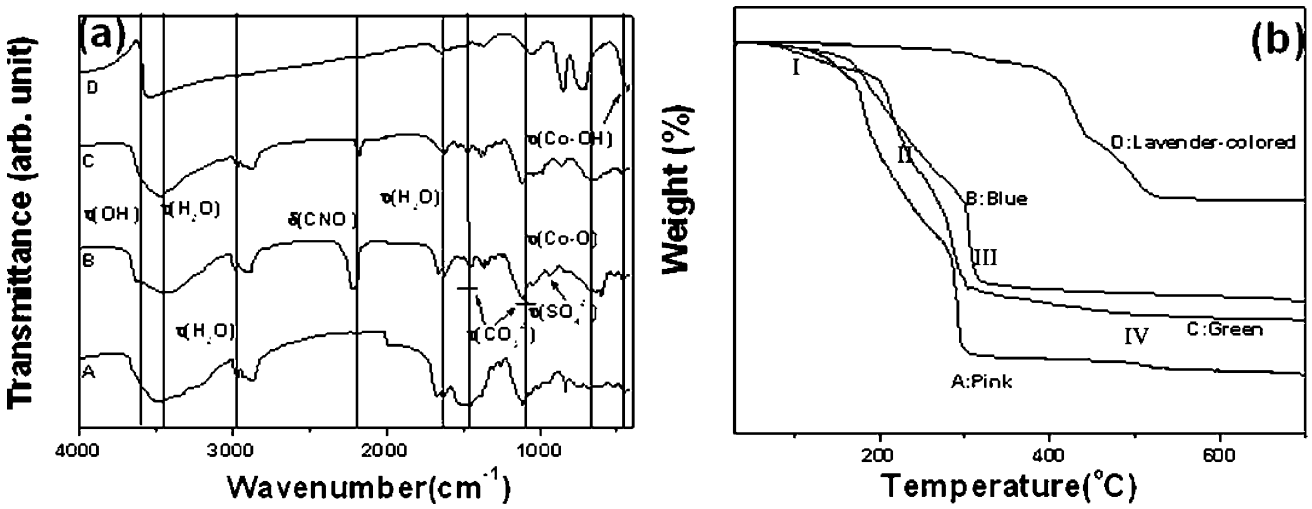

Figure 2. (a) FT−IR and (b) TGA curves for four as-prepared samples of different colors.

the XRD patterns of the four samples obtained at different synthetic conditions. Curve A is the XRD pattern of the pink sample, and all of the diffraction peaks can be perfectly indexed to cobalt chloride carbonate hydroxide hydrate, $Co(OH)_{1.10}Cl_{0.2}$-$(CO_3)_{0.35}\cdot 1.74H_2O$ (JCPDS 38-0547). No impurities can be detected in this pattern, which indicates that pure $Co(OH)_{1.10}Cl_{0.2}$-$(CO_3)_{0.35}\cdot 1.74H_2O$ can be obtained under the current synthesis condition. The XRD result suggests that, in this case, the contents contain only divalent cobalt without any oxidation leading to trivalence because of the low solubility of oxygen in water. Cl^- anion in the solution is incorporated into the precipitates to form chloride-containing cobalt−hydroxide−carbonate compound because of its complexation ability with cobalt. Curve B is the XRD pattern of the blue sample, which shows typical hydrotalcite-like features. The two prominent low-angle reflections at 7.137 Å and 3.563 Å can be assigned to 003 and 006 reflections of the hydrotalcite-like phase (unit cell with three slabs). It can be also found that the *d*-values of three main peaks are correlated: $d_{003} \approx 2d_{006} \approx 3d_{009}$. Taking into consideration its blue color, therefore, this product can be rationally identified as SO_4^{2-}-intercalated α-$Co(OH)_2$. In addition, the *hkl* reflections are not only sharp but also symmetric, distinctly differing from the typical broad "saw-tooth" reflections of the as-reported turbostratic structures of hydrotalcite-like phase, indicating that the produced material is well crystallized.[16] According to the literature, the cell constant *c* is commonly calculated as $c = 3d_{003}$, assuming a 3R polytipism for the hydrotalcite, while the value of cell constant *a* is calculated as $a = 2d_{110}$.[17] So, the lattice parameters of the as-prepared hydrotalcite-like phase are refined to be $a = 3.07$ Å and $c = 21.41$ Å. The larger *d* spacing of the hydrotalcite-like phase is due to the presence of interlamellar anions to preserve charge neutrality and intercalated water molecules. Cl^- is absent in the synthesized product maybe because SO_4^{2-} is preferable and more strongly held in the interlayer than Cl^- because of its larger charge density although Cl^- exists in the precursor ($CoCl_2\cdot 6H_2O$).[20] On the basis of the results of chemical analysis and thermogravimetric measurement, the composition of the as-prepared blue sample is estimated to be $Co(OH)_{1.82}(SO_4)_{0.09}\cdot 1.37H_2O$. Similarly, as shown in curve C of Figure 1, the green sample also shows hydrotalcite-like characteristics. The XRD pattern exhibits prominent reflections at 7.892, 3.946, 2.702, 2.653, and 1.543 Å. The low-angle peak at 7.892 Å can be assigned to the (003) diffraction of the hydrotalcite-like structure, and the peaks at 3.946 Å and 2.653 Å can be assigned to the (006) and (009) diffraction peaks. It can be shown that the *d*-values of the as-prepared sample are related, $d_{003} \approx 2d_{006} \approx 3d_{009}$, in accordance with the hydrotalcite-like structure. This product can be identified as Cl^--intercalated α-$Co(OH)_2$. The lattice parameters of the as-prepared green hydrotalcite-like phase were calculated to be $a = 3.08$ Å and $c = 23.68$ Å. According to the results of chemical analysis and thermogravimetric measurement, the composition of the as-prepared green sample is estimated to be $Co(OH)_{1.81}Cl_{0.19}\cdot 1.12H_2O$. Furthermore, for blue and green samples, XRD patterns obtained from the as-prepared fresh sample and the sample aged in an air atmosphere at room temperature for 6 months show the same curve profile, which indicates that as-prepared sample is air-stable. Curve D is the XRD pattern of the lavender-colored sample. All of the diffraction peaks can be indexed to cobalt hydroxychloride, $Co_2(OH)_3Cl$, with lattice parameters $a = 6.808$ Å and $c = 14.558$ Å (JCPDS 73-2134). The structure of $Co_2(OH)_3Cl$ comprises a close packing of $(OH)_3Cl$ in which Co^{2+} occupies the octahedral sites.[21] The formula $Co_2(OH)_3Cl$ was established by Feitkneeht (1935) for the lavender-colored cobalt hydroxychloride, but only a few studies have been made on this compound.[21]

FT−IR and Thermogravimetric Analysis of Cobalt Basic Salts. FTIR and TGA investigation also affirms the formation of cobalt basic salts. In Figure 2a are shown the Fourier transformation infrared spectra (FT−IR) of the four cobalt basic salt samples (A, pink; B, blue; C, green; D, lavender), ranging from 4000 to 400 cm^{-1}. The spectra for the four samples have the same vibration bands at ca. 3600 cm^{-1}, 1615 cm^{-1}, 668 cm^{-1}, and 446 cm^{-1}. The band at around 3600 cm^{-1} is attributed to the stretching vibration of O−H bond, ν(OH), which indicates the presence of hydroxyl ions because of metal−OH layer in the crystal. The peak at around 1615 cm^{-1} is due to the stretching and bending mode of the water molecules attached to the sample. The absorptions at low-frequency region below 1000 cm^{-1} are ascribed to Co−O stretching (668 cm^{-1}) and Co−OH bending (446 cm^{-1}) vibrations. However, distinct differences can also be seen between four samples in the FT−IR spectra. The large band centered at around 3450 cm^{-1} is observed for pink, blue, and green samples but not for lavender-colored sample, which is assigned to the O−H stretching modes of interlayer water molecules, suggesting the absence of interlayer water molecules in the lavender-colored sample ($Co_2(OH)_3Cl$). Similarly, a shoulder at around 2973 cm^{-1} from hydrogen bonding in the interlayer also indicates the presence of interlayer water molecules in pink, blue, and green samples, but the lavender-colored sample does not show this adsorption.[22]

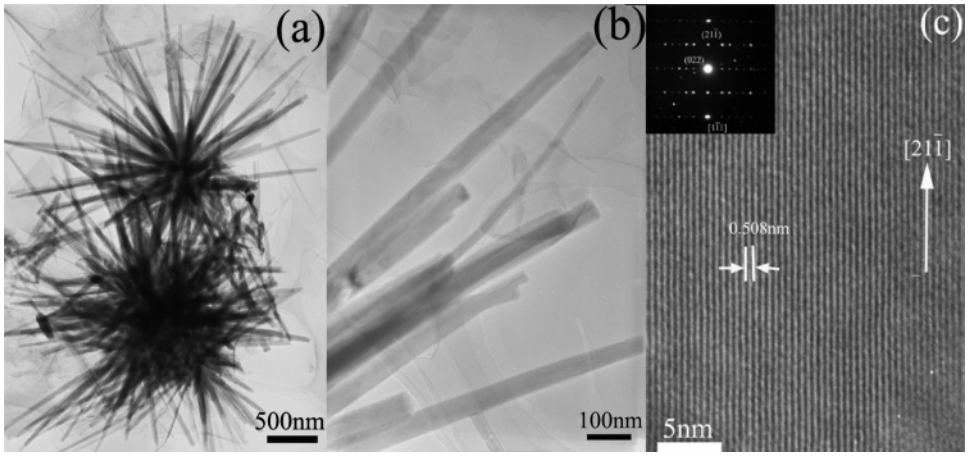

Figure 3. (a, b) TEM images, (c) HRTEM image, and SAED pattern (the inset in c) for the pink sample.

For the blue and green samples, the absorption bands at around 2220 cm^{-1} and 1108 cm^{-1} are attributed to the existence of free NCO^- and CO_3^{2-} ions, which are the products of urea hydrolysis, and therefore can be expected to be included in the sample during synthesis.[12] For the pink sample, the strong absorption bands at 1470 cm^{-1} can be indexed to the υ_3 mode of CO_3^{2-} ions. The other bands at 1106, 831, and 743 cm^{-1} are characterized to the υ_1, υ_2, and υ_4 modes of the carbonate ion, respectively. From the FT−IR spectra, we also can see that the blue sample has an absorption band at about 940 cm^{-1} for the SO_4^{2-} functional group, indicating the incorporation of SO_4^{2-} ions.[23]

Figure 2b shows the TGA curves of the four samples in the temperature range of 30−700 °C. All the peaks in the XRD patterns (not shown here) of the end product after TGA measurements can be indexed to the spinel Co_3O_4. The first three undergo weight loss in four steps over this temperature range as indicted by I, II, III, and IV on the graph with different weight loss, that is 43.7% (expected value: 41.43%), 33.6% (expected value: 34.83%), and 35.0% (expected value: 31.16%), respectively. The mismatch between the observed and expected loss is mainly due to the adsorbed water. I: The weight loss below 180 °C is ascribed to the removal of the adsorbed water. II: The weight loss between 180 °C and 280 °C is assigned to the evaporation of the intercalated water molecules, which is 24.3%, 18.8%, and 19.0%, respectively, roughly in agreement with the expected value on the basis of the estimated formula. III: The weight loss ranging from 280 °C to 320 °C is associated with the loss of water produced by dehydroxylation of the hydroxide layers. Finally, the weight loss after 320 °C can be attributed to the loss of anionic species and transformation to Co_3O_4. The TGA curve of lavender-colored cobalt hydroxychloride shows a distinctly different profile (curve D). No weight loss is found in the range between 30 °C and 250 °C because of the absence of interlayer water molecules. This basic salt decomposes between 250 °C and 390 °C, yielding a mixture of Co_3O_4 and $CoCl_2$. Furthermore, it completely decomposes between 390 °C and 500 °C into Co_3O_4 that remains stable up to 700 °C. It can be formally explained using the following reaction:[24]

$$Co_2(OH)_3Cl \xrightarrow[250\text{-}390^\circ C]{+1/8\ O_2} 1/2\ CoCl_2 + 1/2\ Co_3O_4 + 3/2\ H_2O$$

$$\xrightarrow[390\text{-}500^\circ C]{+1/6\ O_2} 2/3\ Co_3O_4 + 1/2\ Cl_2\uparrow \qquad (2)$$

Morphology of Cobalt Basic Salts. The morphologies and structure of the as-prepared solids were examined with TEM, SAED, HRTEM, and SEM. Figure 3a−c displays the representative TEM images of the pink chloride-containing cobalt−hydroxide−carbonate sample. The TEM images suggest that the 3D urchinlike architecture ranging from 3 to 7 μm in diameter consists of many nanorods with a radial-arranged assembly. These images also reveal that the nanorods are about 20∼40 nm in diameter and 1∼3 μm in length. Each nanorod with a smooth surface has a uniform diameter along its entire length, indicating the good size control by our method. Also, all nanorods protrude from a center point, looking like an urchin. The HRTEM image recorded from an individual nanorod shown in Figure 3c clearly shows that the spacing between any two adjacent lattice fringes is 0.508 nm which matches that of the (011) planes of $Co(OH)_{1.10}Cl_{0.2}(CO_3)_{0.35}\cdot 1.74H_2O$, and the growth direction is revealed to be [21$\bar{1}$] direction. The inset in Figure 3c is the corresponding SAED pattern of the nanorod taken along [1$\bar{1}$1] zone axis. Both the HRTEM image and the SAED pattern show the single-crystalline quality of the as-grown cobalt chloride carbonate hydroxide hydrate nanorods.

Figure 4a and b shows representative SEM images of 3D flowerlike cobalt hydroxysulfate nanostrutures (blue sample), which reveal that a flowerlike architecture consists of 10 or more nanosheets. Some nanosheets as in Figure 4a have irregular shapes with lateral dimension of about 3 × 10 μm, and some nanosheets as in Figure 4b have a rectangular shape with lateral dimension of about 1 × 3 μm. The thickness of these nanosheets is estimated to be about 100−200 nm from SEM observation. Figure 4c shows TEM image of a single nanosheet. The corresponding HRTEM image recorded from an individual nanosheet (Figure 4d) clearly shows the well-resolved interference lattice fringe of about 0.216 nm that corresponds to the (107) crystal plane of hydrotalcite-like phase. The SAED pattern of the nanosheet (the inset in Figure 4d), which was taken along the [010] zone axis, shows the single-crystalline quality of the as-grown cobalt hydroxysulfate nanosheets.

The morphologies of the green Cl^--intercalated α-$Co(OH)_2$ and lavender-colored cobalt hydroxychloride are similar. Figure 5a is a representative SEM image of the lavender-colored sample, which shows that the as-prepared sample has a lamellar structure. From the TEM image (Figure 5b), it can be seen that the lamellar structures are curled and overlapped with each other, forming black edges in the images. Similar nanostructures of TiO_2 were obtained from the layered titanate by the removal of ammonia and water in the interlayer spacing at 350 °C, and the TiO_2 nanostructure possesses a high specific surface area

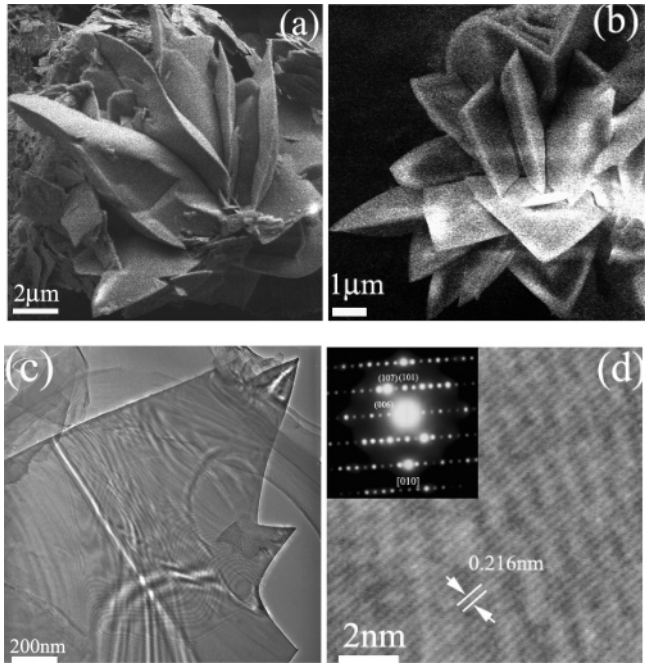

Figure 4. (a, b) SEM images, (c) TEM, and (d) HRTEM image of the blue sample.

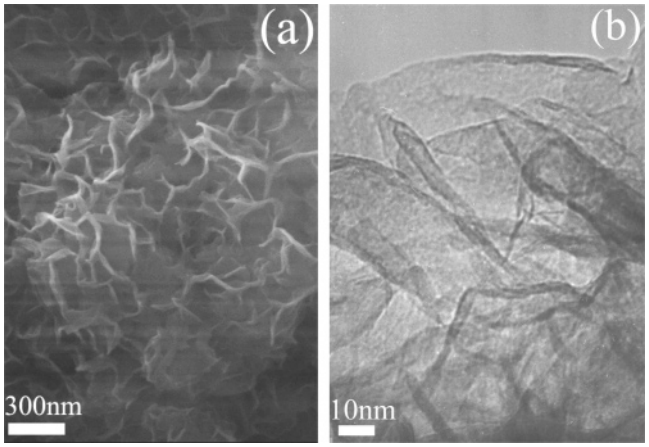

Figure 5. (a) SEM and (b) TEM images for the lavender-colored sample.

(420 m^2 g^{-1}), which is advantageous for a wide variety of practical applications.[25] The difference in product morphologies may be related to the crystal structure of different cobalt basic salt nanostructures. Xu et al. stated that the carbonate anions may act as an inhibitor that selectively decreases the rate of crystal growth in the direction of the side planes of the rod.[10] Thus, it is considered that the inhibition of CO_3^{2-} causes the rodlike growth in the pink sample. The other three samples, which are grown in a sheet form, derive from the layered crystal structure without any CO_3^{2-} inhibition.[15]

Conclusions

Four different kinds of cobalt basic salt have been synthesized in the presence of block polymer P123 by a facile method under mild conditions using nontoxic and inexpensive reagents such as cobalt chloride hexahydrate and urea. The product can be selectively controlled by carefully adding a certain amount of Li_2SO_4 or LiCl. The amount of urea also plays a critical role in the synthesis of cobalt basic salts with different phases. More importantly, two of them exhibit 3D self-assembled architectures. The chloride-containing cobalt−hydroxide−carbonate has an urchinlike morphology which consists of nanorods with 20∼40 nm in diameter and 1∼3 μm in length; the blue cobalt hydroxysulfate has a flowerlike morphology which consists of irregular nanosheets with lateral dimension of about 3×10 μm or rectangular nanosheets of about 1×3 μm. The difference in the crystal structure may result in the difference of morphologies. This synthetic method is simple and controllable and offers great opportunities for bulk synthesis of 3D self-assembled cobalt basic salt nanostructures. It is also expected that the present method may be generalized to synthesize nickel hydroxides and many other hydroxides. The potential applications of the four cobalt basic salt nanostructures, especially in anion exchangers, magnetic cells, and electrodes for alkaline secondary cells, and the relationship between the morphology and properties are being studied.

Acknowledgment. The authors thank Mr. F. Garnier for SEM observations and Drs. D. W. Wang, G. Liu, and Mr. K. Y. Hu for TEM observations. This work was supported by the National Natural Science Foundation of China (Nos 50025204 and 50202013).

References and Notes

(1) Cölfen, H.; Antonietti, M. *Angew. Chem., Int. Ed.* **2005**, *44*, 5576.

(2) Yu, S. H.; Cölfen, H. *J. Mater. Chem.* **2004**, *14*, 2124.

(3) Antonietti, M.; Breulmann, M.; Göltner, C. G.; Cölfen, H.; Kim, K. W.; Walsh, D.; Mann, S. *Chem. Eur. J.* **1998**, *4*, 2493.

(4) Viravaidya, C.; Li, M.; Mann, S. *Chem. Commun.* **2004**, *14*, 2182.

(5) Yu, S. H.; Antonietti, M.; Cölfen, H.; Hartmann, J. *Nano Lett.* **2003**, *3*, 379.

(6) Li, M.; Schnablegger, H.; Mann, S. *Nature* **1999**, *402*, 393.

(7) Yu, S. H.; Cölfen, H.; Xu, A. W.; Dong, W. F. *Cryst. Growth Des.* **2004**, *4*, 33−37.

(8) Elumalai, P.; Vasan, H. N.; Munichandraish, N. *J. Power Sources* **2001**, *93*, 201.

(9) Zhu, Y. C.; Li, H. L.; Koltypin, Y.; Gedanken, A. *J. Mater. Chem.* **2002**, *12*, 729.

(10) Xu, R.; Zeng, H. C. *J. Phys. Chem. B* **2003**, *107*, 12643.

(11) Kamath, P. V.; Therese, G. H. A.; Gopalakrishnan, J. *J. Solid State Chem.* **1997**, *128*, 38.

(12) Ramesh, T. N.; Rajamathi, M.; Kamath, P. V. *J. Solid State Chem.* **2006**, *179*, 2386.

(13) Klissurski, D.; Uzunova, E. *Chem. Mater.* **1991**, *3*, 1060.

(14) Xu, R.; Zeng, H. C. *Chem. Mater.* **1999**, *11*, 67.

(15) Hosona, E.; Fujihara, S.; Honma, I.; Zhou, H. *J. Mater. Chem.* **2005**, *15*, 1938.

(16) Liu, Z. P.; Ma, R. Z.; Osada, M. R.; Takada, K.; Sasaki, T. *J. Am. Chem. Soc.* **2005**, *127*, 13869.

(17) Liu, B. H.; Yu, S. H.; Chen, S. F.; Wu, C. Y. *J. Phys. Chem. B* **2006**, *110*, 4039.

(18) Jeevanandam, P.; Koltypin, Y.; Gedanken, A. *Nano Lett.* **2001**, *1*, 263.

(19) Shi, H. T.; Qi, L. M.; Ma, J. M.; Cheng, H. M.; Zhu, B. Y. *Adv. Mater.* **2003**, *15*, 1647.

(20) Auerbach, S. M.; Carrado, K. A.; Dutta, P. K. *Handbook of layered materials*; Marcel Dekker: New York, 2004; p 373.

(21) Wolf, P. M. *Acta Crystallogr.* **1953**, *6*, 359.

(22) Christian, H.; Hansen, B. *J. Solid State Chem.* **1994**, *113*, 46.

(23) Cloutis, E. A.; Hawthorne, F. C.; Merzman, S. A.; Krenn, K.; Craig, M. A.; Marcino, D.; Methot, M.; Strong, J.; Mustard, J. F.; Blaney, D. L.; Bell, J. F.; Vilas, F. *Icarus* **2006**, *184*, 121.

(24) Garcia-Martinez, O.; Millan, P.; Rojas, R. M.; Torralvo, M. J. *J. Mater. Sci.* **1988**, *23*, 1334.

(25) Takezawa, Y.; Imai, H. *Small* **2006**, *2*, 390.